Available online at www.sciencedirect.com

SCIENCE DIRECT

Virology 338 (2005) 69 – 80

VIROLOGY

www.elsevier.com/locate/yviro

Evidence for an association between heat shock protein 70 and the respiratory syncytial virus polymerase complex within lipid-raft membranes during virus infection

Gaie Brown[a], Helen W. McL. Rixon[a], John Steel[a], Terence P. McDonald[a], Andrew R. Pitt[b], Susan Graham[a], Richard J. Sugrue[a,*]

[a]MRC Virology Unit, Institute of Virology, University of Glasgow, Church Street, Glasgow G11 5JR, UK
[b]The Sir Henry Wellcome Functional Genomics Facility, Joseph Black Building, University of Glasgow, Glasgow G12 8QQ, UK

Received 2 February 2005; returned to author for revision 15 March 2005; accepted 3 May 2005
Available online 3 June 2005

Abstract

In this report, the interaction between respiratory syncytial virus (RSV) and heat shock protein 70 (HSP70) was examined. Although no significant increase in total HSP70 protein levels was observed during virus infection, analysis of the HSP70 content in lipid-raft membranes from mock- and virus-infected cells revealed an increase in the levels of raft-associated HSP70 during virus infection. Fluorescence microscopy demonstrated that this transport of HSP70 into lipid-raft membranes correlated with the appearance of HSP70 within virus-induced inclusion bodies. Furthermore, co-localisation of HSP70 with the virus N protein and the raft lipid GM1 was observed within these structures. Immunoprecipitation experiments demonstrated the ability of HSP70 to interact with the virus polymerase complex in lipid-rafts in an ATP-dependent manner. Collectively, these data suggest that RSV may induce cellular changes which allow the recruitment of specific host-cell factors, via lipid-raft membranes, to the polymerase complex.

Keywords: Respiratory syncytial virus; Virus polymerase complex; NS2 protein; Lipid-raft; HSP70; Proteomics

Introduction

Respiratory syncytial virus (RSV) infection can cause severe bronchiolitis in infants and in certain high-risk groups within the adult population, such as the elderly and immunocompromised. The mature, infectious, RSV particle comprises a ribonucleoprotein (RNP) core that is formed by the interaction of the viral genomic RNA with the nucleocapsid (N) protein, the phosphoprotein (P) and the large (L) protein. The minimal functional polymerase complex requires an association of the N, P and L proteins (Collins et al., 1996; Grosfeld et al., 1995; Yu et al., 1995) but an additional virus protein, M2-1, is required for efficient transcription of the virus genome by the polymerase complex (Fearns and Collins, 1999; Hardy and Wertz, 1998; Hardy et al., 1999; Mason et al., 2003). A lipid envelope, derived from the host cell in which the virus glycoproteins are embedded, surrounds the RNP. An additional virus protein, the matrix (M) protein, which has been shown to regulate virus transcriptional activity (Ghildyal et al., 2002; Rodriguez et al., 2004), is located between the virus envelope and the RNP (Arslanagic et al., 1996; Bachi and Howe, 1973; Brown et al., 2002a; Norrby et al., 1970; Parry et al., 1979; Roberts et al., 1995). During virus replication, the proteins that form the polymerase complex are distributed both within virus filaments and cytoplasmic inclusion bodies (IBs), with the IBs being the major site of accumulation of these proteins in the infected cell. The formation of IBs during virus infection is a feature that is common to several different paramyxoviruses, suggesting that these structures form an integral part of the virus replication strategy.

* Corresponding author. Fax: +44 141 337 2236.
E-mail address: r.sugrue@vir.gla.ac.uk (R.J. Sugrue).

0042-6822/$ - see front matter © 2005 Elsevier Inc. All rights reserved.
doi:10.1016/j.virol.2005.05.004

Interactions among the individual proteins that constitute the virus polymerase complex have been increasingly characterised (reviewed in Easton et al., 2004) and a requirement for cellular protein factors for virus polymerase activity has been demonstrated (Barik, 1992; Bitko et al., 2003; Burke et al., 1998, 2000; Huang et al., 1993; Ulloa et al., 1998). Recent evidence has suggested that during virus replication, the virus polymerase associates with cellular membranes that exhibit detergent-solubility properties that are characteristic of lipid-rafts (Mason et al., 2004; McDonald et al., 2004). In vitro studies have shown that this membrane-association is not required for enzymatic activity since the activity is retained following the membrane solubilisation (Mason et al., 2004). However, this membrane-association may play a role in the recruitment of various factors that are required by the polymerase complex during virus infection. This report demonstrates that at least one host-cell factor, the chaperone heat shock protein 70 (HSP70), is recruited into lipid-raft membranes during virus replication. Furthermore, this recruitment correlates both with a direct interaction between HSP70 and the virus polymerase complex within lipid-raft membranes and with the association of HSP70 and IBs. Our results suggest that cellular changes occur during RSV infection which allow the transport of specific cellular factors to lipid-raft membranes where the virus polymerase complex is located.

Results and discussion

HSP 70 is recruited into lipid-raft membranes during virus infection

The study of lipid-raft membranes from virus-infected cells by two-dimensional nanoflow liquid chromatography mass spectrometry (2D-nLC-MSMS) has been reported previously (McDonald et al., 2004). Using this method, the host-cell protein content of these structures was shown to be qualitatively similar in both mock- and virus-infected samples. However, the results did not indicate whether the levels of these proteins changed upon virus infection and therefore lipid-rafts from mock- and virus-infected cells were analysed further in an attempt to quantitate these protein levels. Total membranes were prepared from mock- and virus-infected Hep2 cells and lipid-rafts prepared as previously described using a flotation gradient (McDonald et al., 2004). Following the 2D-nLC-MSMS analysis, the host-cell protein content was examined in more detail by comparing the abundance of identical peptides in the raft-fractions from mock- and virus-infected cells. This analysis showed that despite failing to detect the presence of additional proteins following virus infection, at least one host cell protein, HSP70, showed an increased abundance. The 2D-nLC-MSMS analysis identified nine different HSP70-specific peptides which were present in the lipid-raft preparations from mock- and RSV-infected cells at sufficient levels and peak resolution to provide reliable data and which showed good coverage of the HSP70 sequence (Fig. 1A). The relative levels of these peptides in the mock- and virus-infected cells were determined by comparing the total ion count peak areas of extracted ion chromatograms normalised to the total ion current (Figs. 1B and C). This analysis showed an approximate four-fold increase of these peptides in lipid-rafts prepared from virus-infected cells compared with those from mock-infected cells, suggesting an increased abundance of HSP70 in lipid-raft membranes following virus-infection. An equivalent analysis of two other cell proteins, PLAP and actin, showed no significant differences between the two preparations (data not shown).

The increased abundance of HSP70 was confirmed by the use of flotation gradient analysis to compare the levels of lipid-raft-associated HSP70 in mock- and in virus-infected cells (Figs. 2A and B). Total membranes from mock- and virus-infected Hep2 cells were treated with 1% Triton X100 at 4 °C, fractionated using a sucrose flotation gradient, and the individual fractions assayed for the presence of HSP70 by Western blotting. In mock-infected cells, high levels of HSP70 were detected, but this was largely confined to the non-raft fractions. Low levels of HSP70 were observed in the lipid-raft fractions (Fig. 2A, highlighted by *) and these results are consistent with a recent report that in non-stressed cells, HSP70 can be detected in lipid-rafts (Broquet et al., 2003). In virus-infected cells, as in mock-infected cells, HSP70 was detected in the non-raft fractions. However, in addition, HSP70 was readily detected in the peak raft fractions (Fig. 2B, highlighted by *). The efficient solubilisation of raft-associated proteins was confirmed by comparing the relative distributions of transferrin receptor (non-raft marker) and caveolin-1 (raft marker), which were found almost exclusively in the non-raft and raft gradient fractions respectively (Figs. 2C and D). Therefore, both the mass spectrometry and flotation gradient analyses suggest that during RSV-infection, there is an increase in the association of HSP70 with lipid-rafts.

It seemed possible that the ability to detect the increased abundance of HSP70 in lipid-rafts during RSV-infection might arise from a generalised increase in HSP70 protein levels during virus infection, which in turn may have allowed the ease of detection of HSP70 in the raft fractions. To discount this possibility, the total level of HSP70 in both mock- and virus-infected cells was compared. In this analysis, whole cell extracts were prepared from mock- and RSV-infected cells and examined by Western blotting using anti-HSP70 (Fig. 3A). This analysis showed that similar levels of a single 70 kDa immunoreactive protein species, the expected size for HSP70, were observed in both mock- and RSV-infected cells. Thus, these data demonstrate that following RSV-infection in Hep2 cells, HSP70 expression levels were not significantly elevated suggesting that the detection of HSP70 in the lipid-raft fractions from virus-infected cells was not a consequence of a generalised increase in HSP70 expression levels following RSV

A

```
  1 MKLSLVAAMLLLLSAARAEEEDKKEDVGTVVGIDLGTTYSCVGVFKNGRV
 51 EIIANDQGNRITPSYVAFTPEGERLIGDAAKNQLTSNPENTVFDAKRLIG
101 RTWNDPSVQQDIKFLPFKVVEKKTKPYIQVDIGGGQTKTFAPEEISAMVL
151 TKMKETAEAYLGKKVTHAVVTVPAYFNDAQRQATKDAGTIAGLNVMRIIN
201 EPTAAAIAYGLDKREGEKNILVFDLGGGTFDVSLLTIDNGVFEVVATNGD
251 THLGGEDFDQRVMEHFIKLYKKKTGKDVRKDNRAVQKLRREVEKAKRALS
301 SQHQARIEIESFYEGEDFSETLTRAKFEELNMDLFRSTMKPVQKVLEDSD
351 LKKSDIDEIVLVGGSTRIPKIQQLVKEFFNGKEPSRGINPDEAVAYGAAV
401 QAGVLSGDQDTGDLVLLDVCPLTLGIETVGGVMTKLIPRNTVVPTKKSQI
451 FSTASDNQPTVTIKVYEGERPLTKDNHLLGTFDLTGIPPAPRGVPQIEVT
501 FEIDVNGILRVTAEDKGTGNKNKITITNDQNRLTPEEIERMVNDAEKFAE
551 EDKKLKERIDTRNELESYAYSLKNQIGDKEKLGGKLSSEDKETMEKAVEE
601 KIEWLESHQDADIEDFKAKKKELEEIVQPIISKLYGSAGPPPTGEEDTAE
651 KDEL
```

B

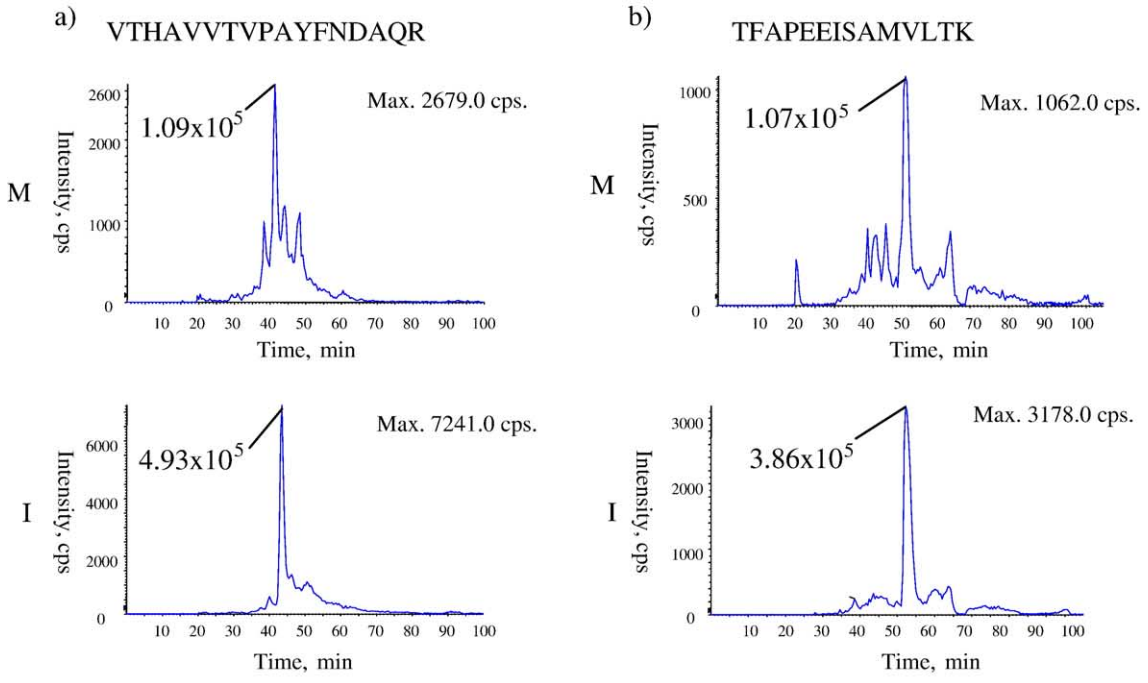

C

PEPTIDES IDENTIFIED	M/Z	AREA VIRUS	AREA MOCK	RATIO
MKETAEAYLGK	414.1	3.8	1.1	3.45
AKFEEELNMDLFR	504.8	4.83	1.63	2.96
AKFEEELNMDLFR	504.9	2.09	0.41	5.10
KSDIDEIVLVGGSTR	530.2	2.52	0.89	2.83
TKPYIQVDIGGGQTK	535.6	3.54	1.10	3.22
VTHAVVTVPAYFNDAQR	629.9	4.93	1.09	4.52
ELEEIVQPIISK	699.3	1.31	0.30	4.37
TFAPEEISAMVLTK	768.8	3.86	1.07	3.61
TFAPEEISAMVLTK	777.3	2.34	0.74	3.16
ITPSYVAFTPEGER	783.7	3.73	0.80	4.66
NQLTSNPENTVFDAKR	839.2	1.12	0.25	4.48
			AVERAGE	3.85
			St Dev	0.79

Fig. 1. Identification by mass spectrometry of sequences that match HSP70 in the lipid-raft fractions isolated from both mock- and RSV-infected cells. (A) Sequence location of matched peptides within HSP70 identified by the 2D-nLC-MSMS analysis. The complete sequence of HSP70 (Accession no. CAB71335) is shown and the peptide sequences identified by mass spectrometry (underlined bold type) are indicated. (B and C) Statistical analysis of HSP70-specific peptides detected in lipid-rafts derived from mock- and virus-infected cells. (B) Examples of chromatograms obtained from two peptides, (a) VTHAVVTVPAYFNDAQR and (b) TFAPEEISAMVLTK isolated from (M) mock- and (I) virus-infected cells are shown. (C) Summary of the statistical analysis for all 11 peptides derived from HSP70 that were selected for analysis. Only peptides showing a significant individual ion score, where the top sequence identified was from HSP70, were chosen.

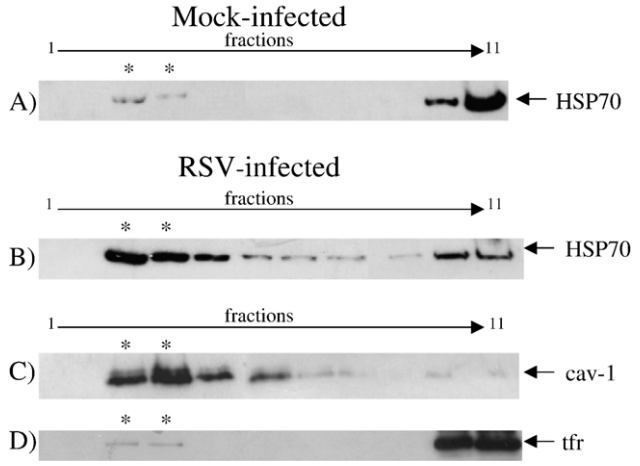

Fig. 2. Flotation gradient analysis of mock- and RSV-infected cell membranes. Membranes were prepared from mock- and virus-infected cells and examined by flotation gradient analysis as described in Materials and methods. Specific proteins were located in gradient fractions by Western blot analysis using relevant antibodies. The distribution of HSP70 in (A) mock- and (B) RSV-infected cells is shown. Also shown is the distribution of the raft-marker caveolin-1 (cav-1) (C) and the non-raft marker transferrin receptor (tfr) (D). 1 is the top fraction and 11 the bottom fraction. The peak raft fractions are indicated (*).

infection. Furthermore, we failed to detect either an increase in HSP70 expression levels or the appearance of higher molecular mass forms of the protein during virus infection. These phenomena are characteristic of the formation of the heat shock-inducible forms of HSP70 suggesting that during virus infection only the constitutively expressed form of the HSP70 was detected. In this manuscript, the constitutive form of protein will be referred to as HSP70. This is consistent with the recent findings of Brasier et al. (2004) who reported that in RSV-infected A459 cells, after an initial increase in mRNA levels (12 h PI), the HSP70 mRNA levels fell during the later stages of the virus replication cycle (16–24 h PI) to below those that were present prior to infection.

HSP 70 associates with the virus-induced inclusion bodies during infection

Confocal microscopy was used to determine whether or not the change in raft-association of HSP70, observed in the flotation gradient analysis, correlated with an alteration in the cellular distribution of HSP70 during virus-infection. The staining pattern of HSP70 and of several RSV proteins located in IBs and virus filaments (e.g., the N, P and M2-1) were compared. In addition, an immunological reagent that specifically recognises the virus NS2 protein was used in this analysis. The N protein is present within both virus filaments and IBs, whereas the NS2 protein is detected within IBs (Weber et al., 1995). The specificity of anti-N has been demonstrated (Murray et al., 2001) and that of anti-NS2, a previously unreported immunological reagent, was demonstrated by Western blotting (Fig. 3B). This antibody recognises a single protein species of 16 kDa in virus-infected cells, which is the reported size for the NS2 protein (Evans et al., 1996). As expected, this protein was not detected in mock-infected cells.

RSV-infected cells were labelled with anti-N and anti-NS2 and the cellular distribution of each protein determined (Figs. 4A–C). Staining of virus-infected cells showed the presence of inclusion bodies (Fig. 4A) as has been described previously (Garcia et al., 1993; Garcia-Barreno et al., 1996). Although the inclusion bodies showed N protein staining across their entirety, the interior of the IBs were more faintly labelled compared to the periphery of the IBs where the stain appeared to accumulate (Fig. 4A, inset), being similar to the previously observed “o-rings” (Garcia et al., 1993). This staining pattern allows two possibilities: either the antibody failed to enter efficiently into the interior of the inclusion body or the staining pattern reflected an increased accumulation of the N protein at the periphery of the IB. This interpretation differs from previously reported work in which the IBs have been examined by electron microscopy. These studies revealed that IBs exist as amorphous structures capable of being labelled by antibodies against the N, P, M2-1 and M proteins (Brown et al., 2002a, 2002b; Garcia et al., 1993; Rixon et al., 2004) but did not provide any evidence for an accumulation of the RNP-associated proteins on the periphery of the IBs. However, a major limitation of this type of approach is that these studies have employed immuno-gold labelling of thin sections, which allows only the detection of antigen exposed on the surface of the section (Hermann et al., 1996). Therefore, an appreciation of the distribution of the viral proteins in IBs using thin sections may not be possible.

In contrast to the staining pattern observed for the N protein, the NS2 antibody appeared to label across the entire interior of the IB structure in a speckled manner. Although the NS2 protein did not appear to be enriched at the periphery of the IB, a small degree of co-localisation between the N and NS2 proteins was seen at this location. This can be seen more clearly in an image in which infected

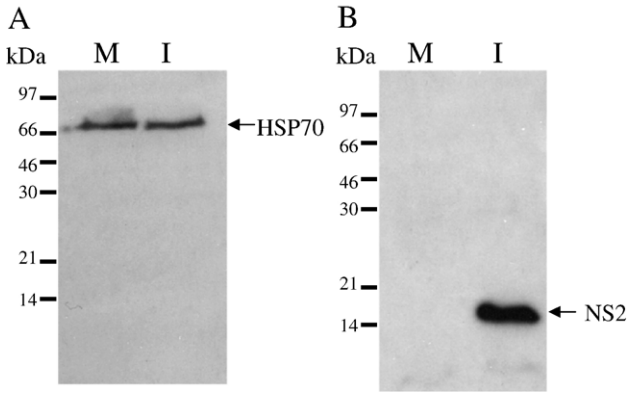

Fig. 3. Western blot analysis of mock- (M) and RSV-infected (I) Hep2 cells at 30 h PI using (A) anti-HSP70 and (B) MAbNS2. The respective protein bands are indicated, as are the positions of the molecular weight markers.

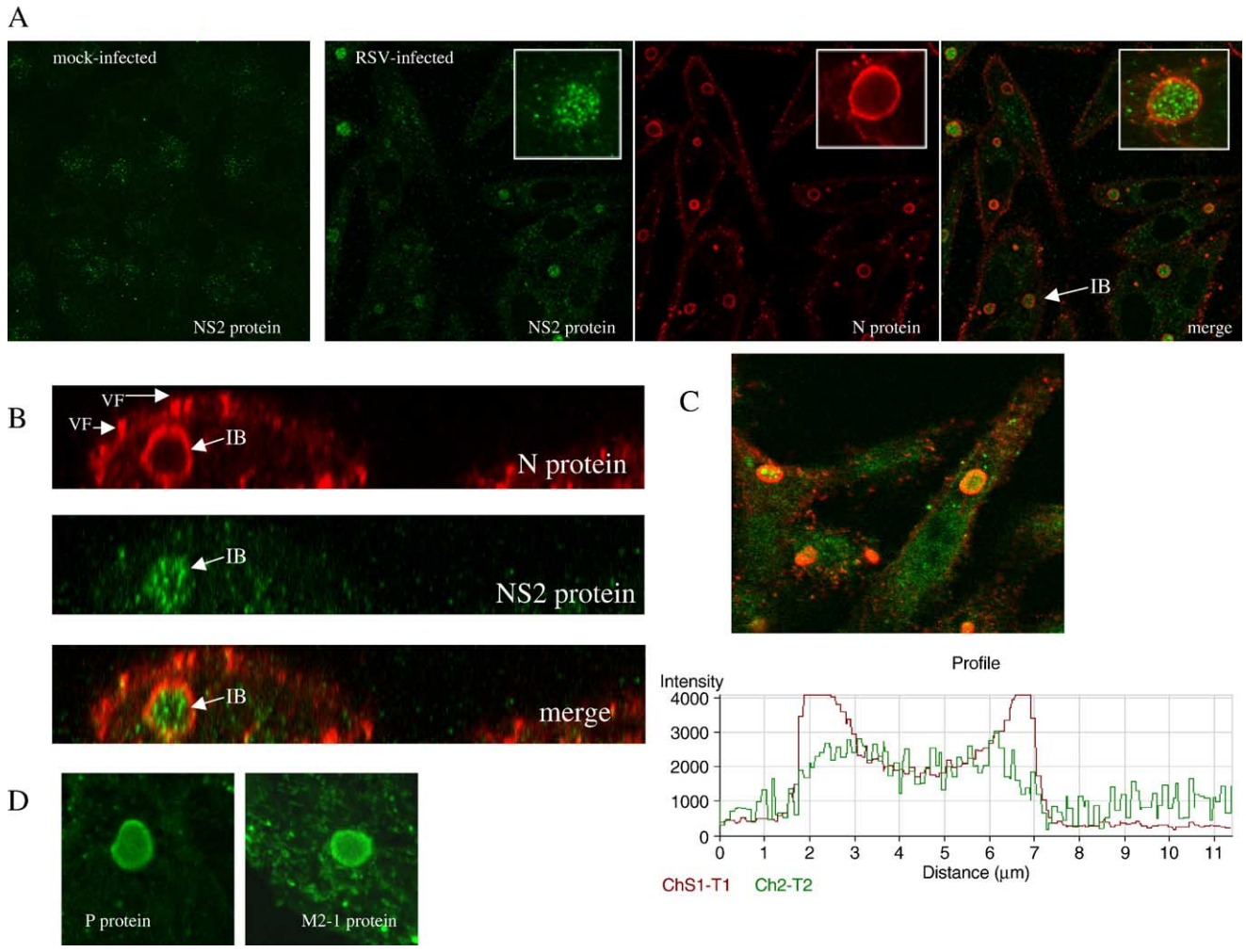

Fig. 4. Examination of the N and NS2 protein distributions in virus-infected Hep2 cells by fluorescence microscopy. (A) Virus-infected cells were labelled with anti-NS2 (green) and anti-N (red) and the distribution of each virus antigen visualised by confocal microscopy. An image from a single optical slice is shown. The IBs are highlighted (white arrow) and insets show enlarged images of single IBs in the single-labelled and merged images. Also shown are mock-infected cells labelled with anti-NS2. (B) Distribution of the NS2 and N protein within IBs in virus-infected cells viewed in cross-section. The images are reconstructed from a z-stack series of images. The distribution of the N protein (red) in relation to the NS2 protein (green) can be seen. The IBs and virus filaments (VF) are highlighted (white arrow). (C) Distribution of the N (red) and NS2 (green) proteins in a single IB shown by densitometry. Low levels of co-localisation between the N and NS2 proteins can be seen as a yellow staining pattern in the merged images. (D) Distribution of the P and M2-1 proteins within IBs.

cells labelled with anti-N and anti-NS2 are viewed in cross section (Fig. 4B). In this case, a speckled pattern throughout the IB can be seen for the NS2 protein, which contrasts with the peripheral staining of the N protein within the IBs. Additionally, analysis of the staining pattern of the N and NS2 proteins by densitometry across a single IB, using the LSM510 software, shows clearly the different distributions of these proteins within the IB (Fig. 4C). The ability to label the entire IB structure with anti-NS2 suggests that the antibody is able to permeate the interior of the IB and the pattern of staining for the N protein may reflect a protein concentration gradient across the IB. A similar type of staining pattern was also observed for the P and M2-1 proteins (Fig. 4D), suggesting that these proteins may, likewise, exhibit a concentration gradient across the IB.

The cellular distribution of HSP70 in mock- and virus-infected cells was compared (Fig. 5A). In mock-infected cells labelled with anti-HSP70, a diffuse staining pattern across the whole cell was observed. However, in virus-infected cells, this staining pattern was also observed, but a second staining pattern was detected in which HSP70 appeared to be sequestered within structures that resemble IBs (Fig. 5A, highlighted by white arrows). This observation is consistent with recent observations where HSP70 appeared to cluster within the cytoplasm of virus-infected A459 cells (Brasier et al., 2004).

The distribution of HSP70 was compared with that of the major RNP-associated proteins, namely the N and P proteins, by examining their staining patterns in virus-infected cells (Figs. 5A and B). HSP70 and the N and P proteins co-localised within the IBs. In addition, anti-HSP70 showed an increase in staining around the periphery of the IBs, as described above for the N protein. Only staining of IBs was observed and no evidence was obtained that HSP70

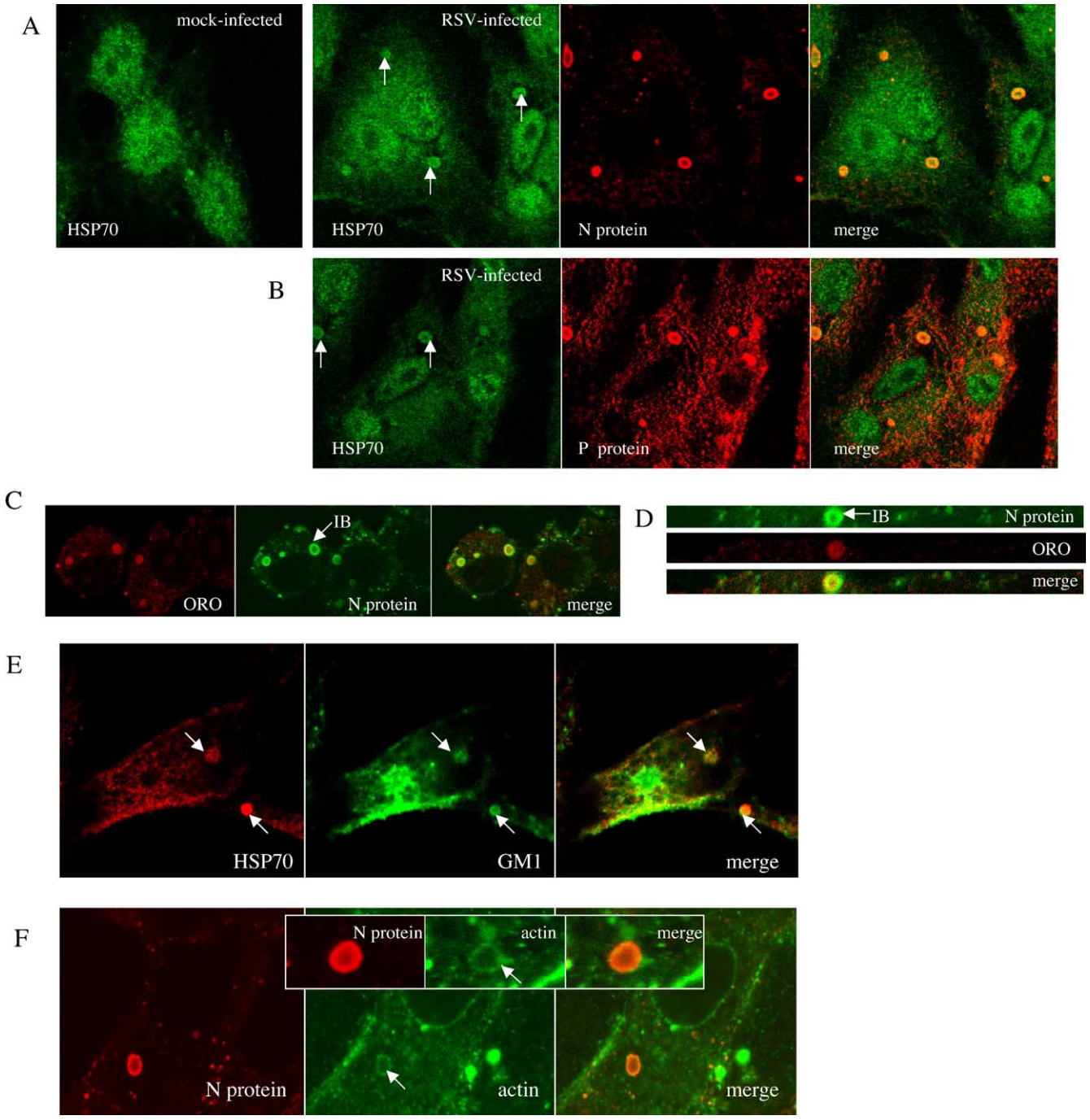

Fig. 5. The distribution of HSP70 in mock- and virus-infected Hep2 cells. Virus-infected cells were labelled with anti-HSP70 and either (A) anti-N or (B) anti-P and the distribution of each antigen visualised by confocal microscopy. The appearance of localised, circular, cytoplasmic HSP70 concentrations is highlighted (white arrows). Also shown are mock-infected cells labelled with anti-HSP70. (C) Virus-infected cells were labelled with anti-N (green) prior to staining with oil-red O (ORO) (red). (D) Distribution of ORO and the N protein within virus-infected cells when viewed in cross-section. Co-localisation between ORO and the N protein is shown by the yellow staining pattern in the merged images. (E) Virus-infected Hep2 cells were incubated at 33 °C with CTX-B-FITC (to detect GM1) and processed for fluorescence microscopy using procedures described previously (Brown et al., 2002b). The treated cells were then labelled with anti-HSP70. The distribution of HSP70 (red) and CTX-B-FITC (green) can be seen and the IBs are highlighted (white arrows). Co-localisation is shown by the yellow staining pattern in the merged images. (F) Actin is present within IBs. Virus infected cells were labelled with anti-N and anti-β actin and the distribution of each antigen visualised. Inset, an enlarged image of a single IB. The presence of the circular staining actin pattern in the IB is highlighted by white arrows.

was present in virus filaments (Brown and Sugrue, data not shown). These data show that during virus-infection, HSP70 is recruited to the sites of accumulation of the major virus structural proteins, i.e., the IBs.

The correlation between HSP70 distribution in the cell and the increased association with lipid-raft membranes suggested that HSP70 was recruited to lipid-rafts present within IBs. The presence of lipids within the IBs can be

demonstrated using the lipid-specific stain, oil-red-O (ORO). This stain is able to detect the accumulation of a variety of different lipids, such as triacylglycerol and cholesterol-esters, in cells. RSV-infected cells were labelled with anti-N prior to staining with ORO (Fig. 5C) as described in Materials and methods. Labelling with anti-N showed, as expected, the presence of IBs and these structures were readily stained with ORO, which can be seen more clearly when the stained cells are viewed in cross-section (Fig. 5D).

In a further analysis, cholera toxin B subunit conjugated to FITC (CTX-B-FITC) was used as a probe to detect the raft lipid, GM1, within the cell. The exposure of cells to CTX-B-FITC under normal culturing conditions allows the internalisation of CTX-B-FITC (Le and Nabi, 2003; Lencer et al., 1992, 1995, 1999) and hence the detection of internal membranes containing GM1. Virus-infected cells were exposed to CTX-B-FITC under these conditions as described previously (Brown et al., 2002b), after which the cells were fixed and then labelled with anti-HSP70 (Fig. 5E). In this way, the distributions of GM1 and HSP70 were compared within the same cell. GM1 (green) and HSP70 (red) exhibited strong co-localisation within IBs, thus providing cytological evidence for an association of HSP70 and GM1 within IBs.

Actin is required for efficient RSV RNA polymerase activity (Burke et al., 1998; Huang et al., 1993) and this host factor has been detected in membrane fractions that are enriched in the virus polymerase complex (Mason et al., 2004; McDonald et al., 2004). We have previously examined RSV-infected cells using phalloidin-FITC (Brown et al., 2002a), a reagent that stabilises actin filaments by binding to the filamentous form of actin (F-actin). Using fluorescence microscopy, the FITC-conjugated form of phalloidin thus allows visualisation of the F-actin distribution in the cell. In this previous analysis, we failed to detect actin staining of either the virus filaments or IBs. However, phalloidin-FITC binds specifically to F-actin and therefore fails to detect other forms of actin, such as globular actin (G-actin), which are also in abundance within the cell. The distribution of actin was therefore examined in infected cells by using an actin antibody whose specificity has been demonstrated in RSV-infected cells (McDonald et al., 2004). Virus-infected cells were labelled with anti-N and anti-actin and the distribution of each antigen visualised by fluorescence microscopy (Fig. 5F). This analysis revealed the presence of actin within the periphery of the IBs providing evidence that host factors that are known to be required for efficient virus polymerase activity are also associated with these structures.

Evidence for an association between the RSV polymerase complex and HSP70

The role played by HSP70 during RSV replication is currently unclear but a role for the protein in the life cycle of several viruses is well established (reviewed in Mayer, 2004). In particular, the recruitment of HSP70 to the sites of transcriptional activity has been shown for several viruses (e.g., herpesviruses, Ohgitani et al., 1998). Previous studies of two paramyxoviruses, measles virus (MV) and the closely-related canine distemper virus (CDV), have provided evidence for an interaction between the N protein and HSP70 (Oglesbee et al., 1989, 1993, 1996; Zhang and Oglesbee, 2003; Zhang et al., 2002), suggesting a possible interaction between HSP70 and the polymerase complex of these viruses. In these cases, HSP70 has been shown to stimulate virus polymerase activity in vitro (Oglesbee et al., 1996; Zhang et al., 2002). It is not clear if HSP70 acts directly as a cofactor in this enzymatic process or if, by binding to the N protein, it allows the N protein, and hence the RNP complex, to fold into a favourable conformation for polymerase activity during virus infection.

The fluorescence microscopy results described above demonstrated a co-localisation between HSP70 and the N protein within IBs and suggested that an interaction may take place between the RSV polymerase complex and HSP70. To examine this possibility, lipid-raft membranes were isolated from mock- and virus-infected cells in the presence (Fig. 6A) or absence (Fig. 6B) of apyrase and subsequently solubilised with non-ionic detergents (1% NP40, 60 mM octyl-β-glucoside). The membrane samples were then immunoprecipitated with anti-N or with a negative control antibody, anti-c-myc and the immunoprecipitates transferred by Western blotting on to PVDF membranes. These membranes were then probed with anti-HSP70 to determine the presence of HSP70 (Figs. 6A, a). The results showed a significant level of HSP70 in samples which were immunoprecipitated from virus-infected cells but not from mock-infected cells. In addition, probing of the membranes with the relevant antibodies revealed the presence of the N, P and M2-1 proteins in the immunoprecipitation assays from virus-infected cells (Figs. 6A, b–d), indicating, as expected, that the various components of the virus polymerase complex co-immunoprecipitated with the N protein. These proteins were not detected in samples that were immunoprecipitated with anti-c-myc or in lysates prepared from mock-infected cells.

The ability to detect HSP70 in the N protein immunoprecipitation assays was dependent upon the presence of apyrase, an enzyme that promotes the dephosphorylation of ATP to ADP and AMP. In the absence of apyrase, the N protein, together with the other virus polymerase-associated proteins, was observed in the immunoprecipitation assays, whereas HSP70 was not detected (Fig. 6B). Apyrase has been used in the analysis of the interaction between the CDV N protein and HSP70 to demonstrate that this is reversible and ATP-dependent (Oglesbee et al., 1996). In these studies, it was envisaged that apyrase stabilised the interaction between the N protein and HSP70, which dissociates in the presence of ATP. The requirement for apyrase suggests also that the interaction between the RSV polymerase complex and HSP70, as in the case of CDV, is both reversible and ATP-dependent.

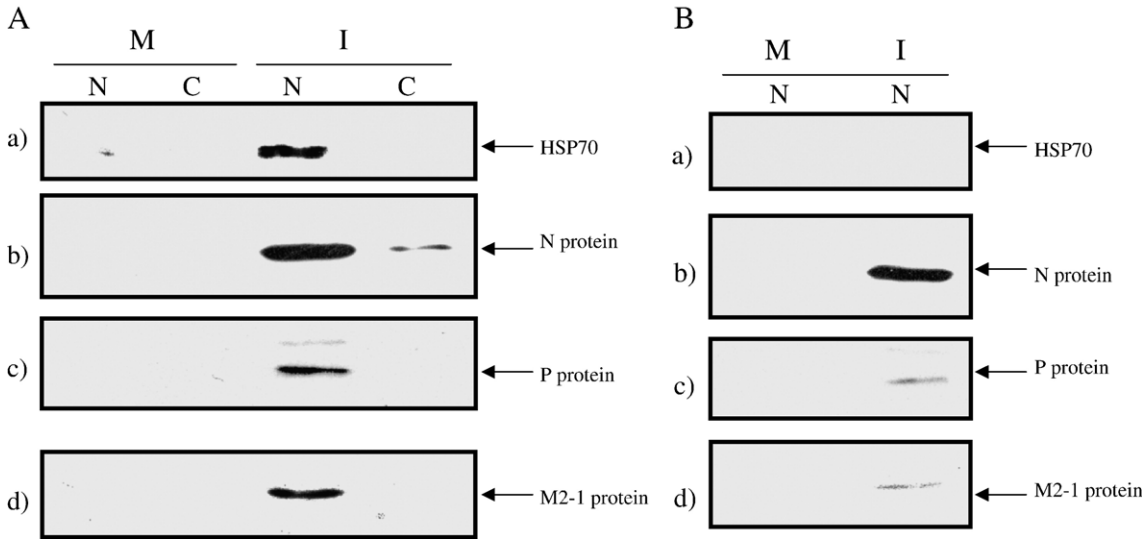

Fig. 6. HSP70 interacts with the RSV polymerase complex within lipid-rafts. Lipid-raft membranes were harvested from (M) mock- and (I) RSV-infected cells in the presence (A) or absence (B) of apyrase. The raft-membrane samples were solubilised with an equal volume of 2% NP40/120 mM octyl-β-glucoside. Aliquots of the solubilised proteins were incubated with protein-A-Sepharose beads (50% slurry) charged either with anti-N (N) or anti-c-myc (C) and incubated o/n at 4 °C. The resin was washed extensively with PBSA +1% Triton X100 at 4 °C and the proteins eluted in boiling mix at 100 °C for 10 min. The proteins were separated by SDS-PAGE and transferred by Western blotting on to PVDF membranes as described in Materials and methods. The membranes were then probed with the relevant antibody (a) anti-HSP70, (b) anti-N, (c) anti-P and (d) anti-M2-1.

The above data provided evidence for an interaction between HSP70 and the virus polymerase complex. However, the possibility existed that this interaction may be a consequence of the recruitment of HSP70 to sites of virus protein expression, perhaps to facilitate correct folding of the newly expressed proteins. Alternatively, it seemed possible that HSP70 could play a direct role in the enzymatic process of the polymerase complex, e.g., acting as a cofactor. Evidence for a direct role was provided by antibody inhibition studies, in which the in vitro effect of anti-HSP70 on virus polymerase activity was examined (Fig. 7). In this analysis, the raft-membranes were pre-incubated with various concentrations of anti-HSP70 prior to assaying for polymerase activity (McDonald et al., 2004). Following the addition of anti-HSP70, a reduction in polymerase activity greater than 50% was observed. In contrast, no significant inhibition in the RNA polymerase activity was observed when the anti-HSP70 was replaced by the addition of equivalent concentrations of either BSA or anti-mouse IgG (data not shown). This finding is similar to that reported previously for CDV and MV and suggests that binding of the antibody to HSP70 may block its interaction with the RSV polymerase complex.

In this analysis, anti-HSP70 concentrations lower than 10 μg/ml resulted in an approximate 10% increase in polymerase activity. This stimulation was not observed when the raft-membranes were incubated with equivalent concentrations of anti-mouse IgG, and the reason for this apparent stimulation in polymerase activity is unknown.

The recruitment of HSP70 into lipid-rafts in response to a variety of different cell stresses has been reported. These stresses include not only heat-shock, but also other conditions such as calcium depletion in the ER and perturbation of protein trafficking. It is envisaged that under conditions of cell stress, heat shock proteins are transported to the cell surface and subsequently secreted by a mechanism that employs lipid-rafts (Broquet et al., 2003). The data show that during RSV-infection, there appears to be a recruitment of HSP70 into lipid-raft membranes that correlates with its redistribution into IBs. The increased abundance of HSP70 in lipid-rafts may arise due to an alteration in the biochemical properties of the secretory

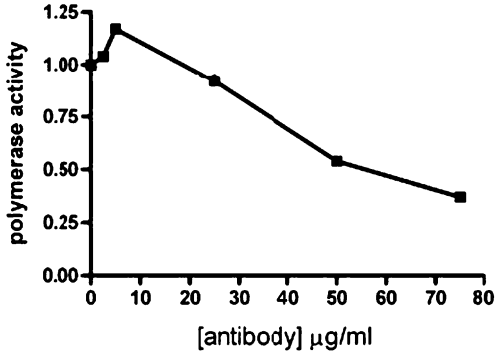

Fig. 7. Inhibition of RSV polymerase activity by anti-HSP70. The RNA polymerase activity in lipid-raft membranes was performed as described previously (McDonald et al., 2004). Lipid-raft membranes from RSV-infected cells were preincubated for 30 min at 4 °C with various concentrations of anti-HSP70 prior to the addition of the polymerase reaction mixture. The polymerase reactions were performed at 37 °C for 45 min and the incorporation of [α-^{32}P]UTP into newly synthesised RNA measured. The polymerase activity is expressed as a fraction of that recorded in the absence of anti-HSP70. Each point on the graph represents the average of 3 individual assays and the standard error within each triplicate assay was less than 5%.

compartments of the cell during RSV infection and IBs form in close proximity to the early compartments of the secretory pathway (McDonald et al., 2004). The direct association of HSP70 with RSV proteins appears to be specific to IBs and no evidence was obtained to suggest that HSP70 was present at the sites of virus assembly (Brown and Sugrue, unpublished observations), which also involve lipid-raft membranes (Brown et al., 2002a, 2002b, 2004; Jeffree et al., 2003; McCurdy and Graham, 2003). This suggests that HSP70 may play a role during virus-infection that relates specifically to IBs.

The precise mechanism involved in the recruitment of HSP70 into IBs during RSV infection is uncertain. It is possible that recruitment is mediated by host factors, as yet unidentified, or that the process is mediated directly by an interaction between HSP70 and components of the virus polymerase complex. In the case of MV, structural studies on the C-terminal domain of the N protein suggest that it is intrinsically disordered and requires an interaction with a partner protein for proper folding (Bourhis et al., 2004; Karlin et al., 2003; Longhi et al., 2003). The binding sites of both the P protein and HSP70 have been mapped to this region of the N protein (Bankamp et al., 1996; Zhang et al., 2002). In the case of the MV N protein, HSP70 has been shown to bind directly to a linear, twenty-four amino acid sequence within this protein (Zhang et al., 2002). This region contains the sequence VYNDRNLL, which conforms to one of the consensus sequences (VYxxR/KxLL, where x is any amino acid) present within certain proteins that interact with HSP70 (Zhang et al., 2002). Such an association may induce folding of this intrinsically disordered region of the N protein and hence influence the activity of the polymerase complex during virus infection.

The interaction between the RSV N and P proteins has been mapped to the C-terminus of the N protein (Garcia-Barreno et al., 1996; Khattar et al., 2000) and it is likely that the interaction between the N and P proteins will have similar consequences for RSV to those described for MV. However, the role played by HSP70 during RSV replication requires further investigation and the nature of the interaction needs to be characterised further. The various components which constitute the polymerase complex of MV and RSV differ significantly (e.g., the physical properties of the RSV and MV N proteins, Bhella et al., 2002). It is possible therefore that the mechanism by which HSP70 and the RSV polymerase complex interacts will differ in detail from that of MV. For example, the HSP70 binding sequence motif described above is not present in the N, P or M2-1 protein sequences from the RSV A2 isolate and a unique motif may be present within these RSV proteins that allows them to interact with HSP70. Additionally, this interaction may involve all the proteins within the polymerase complex rather than any one specific protein as suggested by the MV and CDV data.

It is not clear to what extent other cell factors may interact with the RSV polymerase complex and it is possible that additional host cell proteins, which are as yet unidentified, may mediate the interaction with HSP70. A recent analysis of the transcriptase complex of vesicular stomatitis virus revealed the presence of elongation factor-1α as well as HSP60 (Qanungo et al., 2004). Such findings in a related paramyxovirus suggest that additional host cell factors may also interact with the RSV polymerase complex.

Although the nature of the interaction between the polymerase complex and HSP70 remains to be characterised, the association of the replication complex with HSP70, and the appearance of HSP70 in IBs during virus-infection, lends further support to the possibility that IBs may represent sites of transcriptional activity. In addition, our data suggest that virus-induced changes in lipid-raft membranes may assist in the recruitment of cellular factors by RSV.

Materials and methods

Cells and viruses

The RSV A2 strain was used throughout this study. Hep2 cells were maintained in Dulbecco's Modified Eagle's Medium (DMEM) supplemented with 10% fetal calf serum (FCS) and antibiotics.

Antibodies and stains

The N, P and M2-1 protein antibodies were obtained from Paul Yeo (MRC Virology Unit, Glasgow, UK). The NS2 protein monoclonal antibody (anti-NS2) was prepared as follows. A branched peptide ($NS2_{112-124}$), corresponding to the C-terminal 13 amino acids (KHTPIIYKYDLNP) of the RSV A2 strain, was synthesised on tetravalent $(Lys)_2$-Lys-β-Ala-Wang resin (Novochem) using standard 9-fluorenylmethoxycarbonyl-solid phase chemistry using an Advanced ChemTech 348 Ω automated peptide synthesiser. The resulting peptide, $NS2_{112-124}$, was coupled to a mouse T-cell epitope from sperm whale myoglobin, (sequence, NKALELFRKDIAAKYKE) using standard procedures. This peptide was used to immunise Balb/c mice and monoclonal antibodies were prepared using standard protocols. The tissue culture medium was harvested from anti-NS2-expressing hybridoma cells, concentrated and filtered through a 0.2-μm filter prior to use. The caveolin-1 (N20), HSP70, anti-β actin and transferrin receptor (tfr) antibodies were purchased from Santa Cruz Biotechnology, Transduction Laboratories, Sigma-Aldrich and Zymed Laboratories respectively.

The oil-red O and cholera toxin B subunit conjugated to FITC (CTX-B-FITC) were purchased from Sigma Aldrich.

Western blotting

Western blotting was performed as described previously (Brown et al., 2002a). Briefly, proteins were separated by

SDS PAGE after which they were transferred by Western blotting on to PVDF membranes. The membranes were washed, blocked with 1% Marvel +0.05% Tween and probed with specific primary antibodies for 1 h. The membranes were then washed, probed either with goat anti-mouse or anti-rabbit IgG (whole molecule) peroxidase conjugate (Sigma) as appropriate and the protein bands visualised using the ECL protein detection system (Amersham). Apparent molecular masses were estimated using Rainbow protein markers (Amersham) in the molecular weight range 14.3–220 kDa.

Immunofluorescence

Cells were seeded on 13 mm glass coverslips and either mock- or RSV-infected and incubated at 33 °C for 30 h. The cells were fixed with 3% paraformaldehyde (PFA) in PBS for 30 min at 4 °C and incubated for 1 h at room temperature with the primary antibody, washed and then incubated for a further 1 h with goat anti-mouse IgG (whole molecule) conjugated to either FITC or Cy5 (1/100 dilution). The stained cells were mounted on slides with Citifluor and visualised using a Zeiss Axioplan 2 confocal microscope. The images were processed using LSM 510 v2.01 software.

Staining of GM1 using cholera toxin-B subunit (CTX-B-FITC) was performed as described previously (Brown et al., 2002b). Briefly, CTX-B-FITC was added to cells (diluted (1/250) in PBSA) for 1 h at 33 °C. The cells were washed with PBSA and then fixed in PFA prior to antibody labelling.

Oil-red O staining of cells was performed as described previously (Hope and McLauchlan, 2000). After labelling of cells with relevant antibodies, the coverslips were briefly rinsed in 60% propan-2-ol followed by incubation with 0.5 ml of 60% propan-2-ol containing 1% oil-red O for 1.5–2 min at room temperature. The coverslips were then briefly rinsed with 60% propan-2-ol, washed with PBS and H_2O and mounted on slides using Citifluor.

Flotation gradient analysis of detergent-insoluble lipid-raft membranes

This was performed as described previously (Rixon et al., 2004). Briefly, Hep2 cells were Dounce homogenised in 10 mM Tris pH 7.4/1 mM $MgCl_2$ in the presence or absence of 10 U/ml apyrase (Sigma) supplemented with an EDTA-free protease-inhibitor mixture (Roche Molecular Biochemicals) at 4 °C. Total cell membranes were harvested by centrifugation and resuspended in 1% Triton X-100, 2 mM EDTA in PBS for 1.5 h at 4 °C. The solubilised membranes were made up to a final concentration of 40% (w/v) sucrose in 10 mM Tris pH 7.4/150 mM NaCl/1 mM EDTA (TNE), placed at the bottom of a centrifuge tube and overlayed successively with 7 ml 35% sucrose and 2 ml 5% sucrose in TNE. After centrifugation at 210,000×*g* for 18 h, the gradient was fractionated and the individual fractions analysed by Western blotting using appropriate antibodies.

Protein determination

Protein concentrations were determined using the 2-D Quant Kit (Amersham Biosciences).

Two-dimensional nanoflow liquid chromatography mass spectrometry (2D-nLC-MSMS)

This was performed essentially as described previously (McDonald et al., 2004). Briefly, the lipid-raft fraction was harvested from the flotation gradient and precipitated in 6% TCA, 60 mM sodium deoxycholate (final concentrations). The pellets were resuspended at a concentration of approximately 5 mg/ml in 100 mM Tris pH 7.5 containing 1% octyl-β-glucoside, 6 M urea and 2 M thiourea and solubilised by sonication (4 × 30 s) with vigorous mixing. The solution was then diluted nine-fold with ammonium bicarbonate containing the appropriate amount of trypsin and the protein digested overnight at 37 °C (Promega modified sequencing grade, porcine, 20 μg per 500 μg of raft protein) in 20 mM ammonium bicarbonate. The samples were acidified with 5% formic acid and cleared by centrifugation (10,000×*g*, 10 min). Approximately 200 μg of solubilised protein was applied to a 2D-nLC-MSMS system (Ultimate, standard configuration, Dionex) connected to a QStar Pulsari electrospray mass spectrometer via a nanoflow source (Protana). Mass spectrometric analysis was performed in IDA mode (AnalystQS software, Applied Biosystems), selecting the four most intense ions for MSMS analysis. A survey scan of 400–1500 Da was collected for 3 s followed by 5 s MSMS scans of 50–2000 Da using the standard rolling collision energy settings. Masses were then added to the exclusion list for 3 min. For identification purposes, peaks were extracted and searched using the Mascot Daemon 2.0 (Matrix Science) search engine and assigned a probability-based Mowse score (Perkins et al., 1999). Extracted ion chromatograms were generated manually in AnalystQS with a 0.2-Da window and peak areas measured using the TurboChrom software (Applied Biosystems) and then normalised between samples based on the total ion count of the complete peptide elution region of the corresponding chromatographic trace.

Acknowledgments

We thank Duncan McGeoch for critical review of the manuscript and John McLauchlan for advice on oil-red O staining of cells. AP is grateful to the Wellcome Trust and BBSRC for providing funds to the SHWFGF. JS was supported by the Commission of European Communities specific RTD programme “Quality of Life and Management of Living Resources,” QLK2-CT-2001-01225, “Towards the design of new potent antiviral drugs: structure-function analysis of Paramyxoviridae RNA polymerase.”

References

Arslanagic, E., Matsumoto, M., Suzuki, K., Nerome, K., Tsutsumi, H., Hung, T., 1996. Maturation of respiratory syncytial virus within HEp-2 cell cytoplasm. Acta Virol. 40, 209–214.

Bachi, T., Howe, C., 1973. Morphogenesis and ultrastructure of respiratory syncytial virus. J. Virol. 12, 1173–1180.

Bankamp, B., Horikami, S.M., Thompson, P.D., Huber, M., Billeter, M., Moyer, S.A., 1996. Domains of the measles virus N protein required for binding to P protein and self-assembly. Virology 216, 272–277.

Barik, S., 1992. Transcription of human respiratory syncytial virus genome RNA in vitro: requirement of cellular factor(s). J. Virol. 68, 6813–6818.

Bhella, D., Ralph, A., Murphy, L.B., Yeo, R.P., 2002. Significant differences in nucleocapsid morphology within the Paramyxoviridae. J. Gen. Virol. 83, 1831–1839.

Bitko, V., Oldenburg, A., Garmon, N.E., Barik, S., 2003. Profilin is required for viral morphogenesis, syncytium formation, and cell-specific stress fiber induction by respiratory syncytial virus. BMC Microbiol. 3 (9) (Electronic publication).

Bourhis, J.M., Johansson, K., Receveur-Brechot, V., Oldfield, C.J., Dunker, K.A., Canard, B., Longhi, S., 2004. The C-terminal domain of measles virus nucleoprotein belongs to the class of intrinsically disordered proteins that fold upon binding to their physiological partner. Virus Res. 99, 157–167.

Brasier, A.R., Spratt, H., Wu, Z., Boldogh, I., Zhang, Y., Garofalo, R.P., Casola, A., Pashmi, J., Haag, A., Luxon, B., Kurosky, A., 2004. Nuclear heat shock response and novel nuclear domain 10 reorganization in respiratory syncytial virus-infected a549 cells identified by high-resolution two-dimensional gel electrophoresis. J. Virol. 78, 11461–11476.

Broquet, A.H., Thomas, G., Masliah, J., Trugnan, G., Bachelet, M., 2003. Expression of the molecular chaperone Hsp70 in detergent-resistant microdomains correlates with its membrane delivery and release. J. Biol. Chem. 278, 21601–21606.

Brown, G., Aitken, J., Rixon, H.W.McL., Sugrue, R.J., 2002a. Caveolin-1 is incorporated into mature RSV particles during virus assembly on the surface of virus-infected cells. J. Gen. Virol. 83, 611–621.

Brown, G., Rixon, H.W.McL., Sugrue, R.J., 2002b. Respiratory syncytial virus assembly occurs in GM1-rich regions of the host-cell membrane and alters the cellular distribution of tyrosine phosphorylated caveolin-1. J. Gen. Virol. 83, 1841–1850.

Brown, G., Jeffree, C.E., McDonald, T., Rixon, H.W.McL., Aitken, J.D., Sugrue, R.J., 2004. Analysis of the interaction between respiratory syncytial virus and lipid-rafts in Hep2 cells during infection. Virology 327, 175–185.

Burke, E., Dupuy, L., Wall, C., Barik, S., 1998. Role of cellular actin in the gene expression and morphogenesis of human respiratory syncytial virus. Virology 252, 137–148.

Burke, E., Mahoney, N.M., Almo, S.C., Barik, S., 2000. Profilin is required for optimal actin-dependent transcription of respiratory syncytial virus genome RNA. J. Virol. 74, 669–675.

Collins, P.L., Hill, M.G., Cristina, J., Grosfeld, G., 1996. Transcription elongation factor of respiratory syncytial virus, a non-segmented negative-strand RNA virus. Proc. Natl. Acad. Sci. U.S.A. 93, 81–85.

Easton, A.J., Domachowske, J.B., Rosenberg, H.F., 2004. Animal pneumoviruses: molecular genetics and pathogenesis. Clin. Microbiol. Rev. 17, 390–412.

Evans, J.E., Cane, P.A., Pringle, C.R., 1996. Expression and characterisation of the NS1 and NS2 proteins of respiratory syncytial virus. Virus Res. 43, 155–161.

Fearns, R., Collins, P.L., 1999. Role of the M2-1 transcription antitermination protein of respiratory syncytial virus in sequential transcription. J. Virol. 73, 5852–5864.

Garcia, J., Garcia-Barreno, B., Vivo, A., Melero, J.A., 1993. Cytoplasmic inclusions of respiratory syncytial virus-infected cells: formation of inclusion bodies in transfected cells that coexpress the nucleoprotein, the phosphoprotein, and the 22K protein. Virology 195, 243–247.

Garcia-Barreno, B., Delgado, T., Melero, J.A., 1996. Identification of protein regions involved in the interaction of human respiratory syncytial virus phosphoprotein and nucleoprotein: significance for nucleocapsid assembly and formation of cytoplasmic inclusions. J. Virol. 70, 801–808.

Ghildyal, R., Mills, J., Murray, M., Vardaxis, N., Meanger, J., 2002. Respiratory syncytial virus matrix protein associates with nucleocapsids in infected cells. J. Gen. Virol. 83, 753–757.

Grosfeld, H., Hill, M.G., Collins, P.L., 1995. RNA replication by respiratory syncytial virus (RSV) is directed by the N, P, and L proteins; transcription also occurs under these conditions but requires RSV superinfection for efficient synthesis of full length mRNA. J. Virol. 69, 5677–5686.

Hardy, R.W., Wertz, G.W., 1998. The product of the respiratory syncytial virus M2 gene ORF1 enhances readthrough of intergenic junctions during viral transcription. J. Virol. 72, 520–526.

Hardy, R.W., Harmon, S.B., Wertz, G.W., 1999. Diverse gene junctions of respiratory syncytial virus modulate the efficiency of transcription termination and respond differently to M2-mediated antitermination. J. Virol. 73, 170–176.

Hermann, R., Walther, P., Muller, M., 1996. Immunogold-labelling in scanning electron microscopy. Histochem. Cell Biol. 106, 31–39.

Hope, R.G., McLauchlan, J., 2000. Sequence motifs required for lipid droplet association and protein stability are unique to the hepatitis C virus core protein. J. Gen. Virol. 81, 1913–1925.

Huang, Y.T., Romito, R.R., De, B.P., Banerjee, A.K., 1993. Characterization of the in vitro system for the synthesis of mRNA from human respiratory syncytial virus. Virology 193, 862–867.

Jeffree, C.J., Rixon, H.W.McL., Brown, G., Aitken, J., Sugrue, R.J., 2003. Distribution of the attachment (G) glycoprotein and GM1 within the envelope of mature respiratory syncytial virus filaments revealed using field emission scanning electron microscopy. Virology 306, 254–267.

Karlin, D., Ferron, F., Canard, B., Longhi, S., 2003. Structural disorder and modular organization in Paramyxovirinae N and P. J. Gen. Virol. 84, 3239–3252.

Khattar, S.K., Yunus, A.S., Collins, P.L., Samal, S.K., 2000. Mutational analysis of the bovine respiratory syncytial virus nucleocapsid protein using a minigenome system: mutations that affect encapsidation, RNA synthesis, and interaction with the phosphoprotein. Virology 270, 215–228.

Le, P.U., Nabi, I.R., 2003. Distinct caveolae-mediated endocytic pathways target the Golgi apparatus and the endoplasmic reticulum. J. Cell Sci. 116, 1059–1071.

Lencer, W.I., Delp, C., Neutra, M.R., Madara, J.L., 1992. Mechanism of cholera toxin action on a polarized human intestinal epithelial cell line: role of vesicular traffic. J. Cell Biol. 117, 1197–1209.

Lencer, W.I., Constable, C., Moe, S., Jobling, M.G., Webb, H.M., Ruston, S., Madara, J.L., Hirst, T.R., Holmes, R.K., 1995. Targeting of cholera toxin and *Escherichia coli* heat labile toxin in polarized epithelia: role of COOH-terminal KDEL. J. Cell Biol. 131, 951–962.

Lencer, W.I., Hirst, T.R., Holmes, R.K., 1999. Membrane traffic and the cellular uptake of cholera toxin. Biochim. Biophys. Acta 1450, 177–190.

Longhi, S., Receveur-Brechot, V., Karlin, D., Johansson, K., Darbon, H., Bhella, D., Yeo, R., Finet, S., Canard, B., 2003. The C-terminal domain of the measles virus nucleoprotein is intrinsically disordered and folds upon binding to the C-terminal moiety of the phosphoprotein. J. Biol. Chem. 278, 18638–18648.

Mason, S.W., Aberg, E., Lawetz, C., DeLong, R., Whitehead, P., Liuzzi, M., 2003. Interaction between human respiratory syncytial virus (RSV) M2-1 and P proteins is required for reconstitution of M2-1-dependent RSV minigenome activity. J. Virol. 77, 10670–10676.

Mason, S.W., Lawetz, C., Gaudette, Y., Do, F., Scouten, E., Lagace, L., Simoneau, B., Liuzzi, M., 2004. Polyadenylation-dependent screening assay for respiratory syncytial virus RNA transcriptase acti-

vity and identification of an inhibitor. Nucleic Acids Res. 32, 4758–4767.
Mayer, M.P., 2004. Recruitment of Hsp70 chaperones: a crucial part of viral survival strategies. Rev. Physiol., Biochem. Pharmacol. (Electronic publication ahead of print).
McCurdy, L.H., Graham, B.S., 2003. Role of plasma membrane lipid microdomains in respiratory syncytial virus filament formation. J. Virol. 77, 1747–1756.
McDonald, T.P., Pitt, A.R., Brown, G., Rixon, H.W.McL., Sugrue, R.J., 2004. Evidence that the respiratory syncytial virus polymerase complex associates with lipid rafts in virus-infected cells: a proteomic analysis. Virology 330, 147–157.
Murray, J., Loney, C., Murphy, L.B., Graham, S., Yeo, R.P., 2001. Characterization of monoclonal antibodies raised against recombinant respiratory syncytial virus nucleocapsid (N) protein: identification of a region in the carboxy terminus of N involved in the interaction with P protein. Virology 289, 252–261.
Norrby, E., Marusyk, H., Orvell, C., 1970. Morphogenesis of respiratory syncytial virus in a green monkey kidney cell line (Vero). J. Virol. 6, 237–242.
Oglesbee, M., Tatalick, L., Rice, J., Krakowka, S., 1989. Isolation and characterization of canine distemper virus nucleocapsid variants. J. Gen. Virol. 70, 2409–2419.
Oglesbee, M.J., Kenney, H., Kenney, T., Krakowka, S., 1993. Enhanced production of morbillivirus gene-specific RNAs following induction of the cellular stress response in stable persistent infection. Virology 192, 556–567.
Oglesbee, M.J., Liu, Z., Kenney, H., Brooks, C.L., 1996. The highly inducible member of the 70 kDa family of heat shock proteins increases canine distemper virus polymerase activity. J. Gen. Virol. 77, 2125–2135.
Ohgitani, E., Kobayashi, K., Takeshita, K., Imanishi, J., 1998. Induced expression and localization to nuclear-inclusion bodies of hsp70 in varicella-zoster virus-infected human diploid fibroblasts. Microbiol. Immunol. 42, 755–760.
Parry, J.E., Shirodaria, P.V., Pringle, C.R., 1979. Pneumoviruses: the cell surface of lytically and persistently infected cells. J. Gen. Virol. 44, 479–491.
Perkins, D.N., Pappin, D.J., Creasy, D.M., Cottrell, J.S., 1999. Probability-based protein identification by searching sequence databases using mass spectrometry data. Electrophoresis 20, 3551–3567.
Qanungo, K.R., Shaji, D., Mathur, M., Banerjee, A.K., 2004. Two RNA polymerase complexes from vesicular stomatitis virus-infected cells that carry out transcription and replication of genome RNA. Proc. Natl. Acad. Sci. U.S.A. 101, 5952–5957.
Rixon, H.W.McL., Brown, G., Aitken, J., McDonald, T., Graham, S., Sugrue, R.J., 2004. The small hydrophobic (SH) protein accumulates within lipid-raft structures of the Golgi complex during respiratory syncytial virus (RSV) infection. J. Gen. Virol. 85, 1153–1165.
Roberts, S.R., Compans, R.W., Wertz, G.W., 1995. Respiratory syncytial virus matures at the apical surfaces of polarized epithelial cells. J. Virol. 69, 2667–2673.
Rodriguez, L., Cuesta, I., Asenjo, A., Villanueva, N., 2004. Human respiratory syncytial virus matrix protein is an RNA-binding protein: binding properties, location and identity of the RNA contact residues. J. Gen. Virol. 85, 709–719.
Ulloa, L., Serra, R., Asenjo, A., Villanueva, N., 1998. Interactions between cellular actin and human respiratory syncytial virus (HRSV). Virus Res. 53, 13–25.
Weber, E., Humbert, B., Streckert, H.J., Werchau, H., 1995. Nonstructural protein 2 (NS2) of respiratory syncytial virus (RSV) detected by an antipeptide serum. Respiration 62, 27–33.
Yu, Q., Hardy, R.W., Wertz, G.W., 1995. Functional cDNA clones of the human respiratory syncytial (RS) virus N, P and L proteins support replication of RS virus genomic RNA analogs and define minimal transacting requirements for RNA replication. J. Virol. 69, 2412–2419.
Zhang, X., Oglesbee, M., 2003. Use of surface plasmon resonance for the measurement of low affinity binding interactions between HSP72 and measles virus nucleocapsid protein. Biol. Proced. Online 5, 170–181 (Electronic publication).
Zhang, X., Glendening, C., Linke, H., Parks, C.L., Brooks, C., Udem, S.A., Oglesbee, M., 2002. Identification and characterization of a regulatory domain on the carboxyl terminus of the measles virus nucleocapsid protein. J. Virol. 76, 8737–8746.